Published in final edited form as:
Mol Microbiol. 2010 January ; 75(1): 92–106. doi:10.1111/j.1365-2958.2009.06959.x.

Potential role for ESAT6 in dissemination of *M. tuberculosis* via human lung epithelial cells

Arvind G. Kinhikar[1,†,‡], **Indu Verma**[2,†], **Dinesh Chandra**[1], **Krishna K. Singh**[1], **Karin Weldingh**[3,§], **Peter Andersen**[3], **Tsungda Hsu**[4], **William R. Jacobs Jr**[4], and **Suman Laal**[1,5,6,*]

[1]Department of Pathology, New York University Langone School of Medicine, New York, USA.

[2]Department of Biochemistry, Post Graduate Institute of Medical Education and Research, Chandigarh, India.

[3]Department of Infectious Disease Immunology, Statens Serum Institute, Copenhagen S, Denmark.

[4]Albert Einstein College of Medicine, Bronx, New York, USA.

[5]Department of Microbiology, New York University Langone School of Medicine, New York, USA.

[6]New York Harbor Health Care System, New York, USA.

Summary

ESAT6 has recently been demonstrated to cause haemolysis and macrophage lysis. Our studies demonstrate that ESAT6 causes cytolysis of type 1 and type 2 pneumocytes. Both types of pneumocytes express membrane laminin, and ESAT6 exhibits dose-dependent binding to both cell types and to purified human laminin. While minimal ESAT6 was detected on the surface of *Mycobacterium tuberculosis* grown *in vitro*, exogenously provided ESAT6 specifically associated with the bacterial cell surface, and the bacterium-associated ESAT6 retained its cytolytic ability. *esat6* transcripts were upregulated ~4- to ~13-fold in bacteria replicating in type 1 cells, and ~3- to ~5 fold in type 2 cells. *In vivo*, laminin is primarily concentrated at the basolateral surface of pneumocytes where they rest on the basement membrane, which is composed primarily of laminin and collagen. The upregulation of *esat6* transcripts in bacteria replicating in pneumocytes, the specific association of ESAT6 with the bacterial surface, the binding of ESAT6 to laminin and the lysis of pneumocytes by free and bacterium-associated ESAT6 together suggest a scenario wherein *Mycobacterium tuberculosis* replicating in pneumocytes may utilize surface ESAT6 to anchor onto the basolateral laminin-expressing surface of the pneumocytes, and damage the cells and the basement membrane to directly disseminate through the alveolar wall.

Introduction

Approximately ~1/3 of the global human population are infected with *M. tuberculosis* (*M. tb*), making it one of the most successful pathogens in the world. Infection with *M. tb* is believed

*For correspondence. suman.laal@nyumc.org; Tel. (+1) 2122634164; Fax (+1) 2129516321..
†These authors are equal contributors.
‡Present addresse: CovX Research LLC, 9381 Judicial Drive, Suite 200, San Diego, USA
§Present addresse: Novo Nordisk Park 1, 2760 Måløv.

Supporting information
Additional supporting information may be found in the online version of this article.
Please note: Wiley-Blackwell are not responsible for the content or functionality of any supporting materials supplied by the authors. Any queries (other than missing material) should be directed to the corresponding author for the article.

to be initiated when an airborne droplet carrying 1–3 bacilli is inhaled into the alveoli and is internalized by alveolar phagocytic cells, the bacteria replicate intracellularly and the bacteria-laden cells cross the alveolar barrier to cause systemic dissemination (Birkness *et al.*, 1999; Teitelbaum *et al.*, 1999; Bermudez *et al.*, 2002; Jiao *et al.*, 2002; Geijtenbeek *et al.*, 2003; Tailleux *et al.*, 2003; Menozzi *et al.*, 2005; Humphreys *et al.*, 2006). This intracellular replication, and the simultaneous dissemination of the pathogen to the pulmonary lymph nodes and to various extrapulmonary sites occurs prior to the elicitation of the adaptive immune responses and is responsible for the extraordinary success of *M. tb* in establishing infection (Chackerian *et al.*, 2002; McMurray, 2003). Although the *M. tb*–phagocytic cell interaction has been intensively investigated, recent studies have demonstrated that *M. tb* can also infect non-phagocytic cells that are present in the alveolar barrier, namely the M cells, as well as the alveolar endothelial and type 2 epithelial cells (McDonough *et al.*, 1995; Teitelbaum *et al.*, 1999; Bermudez *et al.*, 2002; Danelishvili *et al.*, 2003; Hsu *et al.*, 2003; Mehta *et al.*, 2006).

Mycobacterium tuberculosis replicates efficiently within type 2 cells and also causes their cytolysis, suggesting that infection of these cells *in vivo* could potentially alter their barrier function (McDonough *et al.*, 1995; Bermudez *et al.*, 2002; Danelishvili *et al.*, 2003). Studies with an *in vitro* model of the alveolar wall comprising of a bilayer of epithelial (A549) and endothelial cells (EAhy926) have demonstrated that *M. tb*-laden macrophages translocate across the bilayer more efficiently when the epithelial cells have been preinfected with *M. tb*, suggesting that damage to the alveolar wall may enhance dissemination of *M. tb* (Bermudez *et al.*, 2002). Interestingly, studies with different mycobacterial strains demonstrated that while both virulent H_{37}Rv tubercle bacilli and BCG infect the type 2 pneumocytes, the latter is attenuated for cytolysis (McDonough *et al.*, 1995; Dobos *et al.*, 2000). Also, *in vitro* studies with the above described alveolar wall bilayer model showed that while both *M. tb* and BCG cross the bilayer by transport within infected mononuclear phagocytes, only the former translocate independently across the bilayer (Bermudez *et al.*, 2002). Together, these studies suggest that *M. tb* infection of the epithelial cells, replication in them and the subsequent disruption may contribute to the dissemination of both free and macrophage-ingested *M. tb* from the lungs.

Comparative studies have identified 16 regions of difference (RD1-16) between the genomes of *M. tb* and BCG, of which one deletion, termed ‘RD1’, is absent from all BCG substrains currently used as TB vaccines globally. RD1 is part of a 15-gene locus (ESX-1), which encodes a secretion system that enables the secretion of several proteins including ESAT6 and CFP10, which are also encoded in RD1. Studies from several different labs have demonstrated that the mutants of RD1 and of individual genes in this region are attenuated for cytolysis of type 2 pneumocytes and macrophages, cell-to-cell spread, pulmonary necrosis and bacterial dissemination from the lungs *in vivo* (Hsu *et al.*, 2003; Lewis *et al.*, 2003; Guinn *et al.*, 2004). ESAT6 was initially reported to cause disruption of conductance and destruction of artificial planal bilayers (Hsu *et al.*, 2003). Recent studies have reported that ESAT6 induces apoptosis of macrophages (Derrick and Morris, 2007) and may contribute to the translocation of *M. tb* from the phagolysosomes to the cytoplasm in myeloid cells (van der Wel *et al.*, 2007). Importantly, ESAT6 has been demonstrated to cause lysis of red blood cells and macrophages by pore formation in their membranes (Smith *et al.*, 2008). Together, these studies suggest that the ESAT6 may contribute to cellular invasion, escape from phagolysosomes, cell-to-cell spread and dissemination of *M. tb* by acting like a cytolytic pore-forming toxin.

The alveolar epithelial surface is covered by both type 1 and type 2 pneumocytes; in fact, the type 1 cells cover > 90% of the alveolar surface, greatly increasing the possibility that the inhaled bacilli will contact these cells (Rennard *et al.*, 1983; Dunsmore and Rannels, 1996). While invasion of and replication in type 2 pneumocytes by *M. tb* resulting in their lysis is well established, the interaction of *M. tb* with type 1 cells has not been investigated. Recent studies

with other respiratory pathogens (*Yersinia pestis* and *Legionella pneumophila*) have shown that they can invade and replicate in the type 1 pneumocyte cell line WI26 (Harb and Kwaik, 2000; Liu *et al.*, 2006; Galvan *et al.*, 2007). Moreover, *Pneumocystis carini* and *Streptococcus pneumoniae* have been shown to preferentially bind to and damage type I cells *in vivo* to achieve dissemination across the alveolar barrier (Nakamura and Wada, 1998; Rubins and Janoff, 1998; Rubins *et al.*, 1998; Kaneshiro, 2001; Garcia-Suarez Mdel *et al.*, 2007). Preliminary studies in our lab confirmed that *M. tb* can invade and replicate in WI26 pneumocytes (Vir *et al.*, 2009). In the current studies, we have investigated the interaction of ESAT6 with both type 1 (WI26) and type 2 (A549) cells. Our results demonstrate that ESAT6 causes cytolysis of both type 1 and 2 pneumocytes. Both cell types express laminin in their membranes and ESAT6 binds to both type 1 and type 2 pneumocytes, as well as to purified human laminin in a dose-dependent manner. The former cells express higher levels of laminin/cell, bind more ESAT6 and are significantly more sensitive to cytolysis. The cytolytic activity of ESAT6 for both cell types is retained when complexed to CFP10. While little ESAT6 could be demonstrated on the cell surface of *M. tb* grown *in vitro*, exogenously provided ESAT6 associates with the cell surface of intact H_{37}Rv, H_{37}Rv*:*Δ*cfp10* and H_{37}Rv*:*Δ*RD1* bacteria and this bacterium-associated ESAT6 retains its cytolytic ability. Transcripts for *esat6* are upregulated in *M. tb* replicating in type 1 and 2 pneumocytes. Together, these studies demonstrate that *M. tb* ESAT6 acts as a cytolytic toxin for pulmonary epithelial cells and suggests a potential mechanism by which ESAT6 may contribute to the phagocyte-independent dissemination of the bacteria from the lungs.

Results

ESAT6 causes cytolysis of type 1 and type 2 pneumocytes

Previous studies demonstrated that H_{37}Rv*:*Δ*RD1*, H_{37}Rv:Δ*esat6*, H_{37}Rv:Δ*cfp10* bacteria that either fail to express or secrete ESAT6 are attenuated for cytolysis of type 2 pneumocytes (Hsu *et al.*, 2003). To determine if purified recombinant ESAT6 and/or CFP10 cause cytolysis of pneumocytes, type 1 (WI26) and type 2 (A549) cells were exposed to several concentrations of ESAT6 and CFP10 ranging from 3 to 15 μg ml^{-1} for 24, 48 and 72 h (Fig. 1A and B). Both type 1 and type 2 pneumocytes demonstrated a time- and dose-dependent cytolysis when exposed to ESAT6 (Fig. 1A and B). At every concentration and time point tested, type 1 pneumocytes were more sensitive to cytolysis as compared with type 2 cells (Fig. 1A–C). In contrast, no cytolysis was observed with CFP10 at any of the concentrations or time points tested (Fig. 1A and B, and data not shown). The cell death was readily observed microscopically, and was specific to ESAT6 since the viability of cells exposed to medium alone, or to other recombinant proteins of *M. tb* (CFP10, Malate synthase (MS) or Superoxide dismutase C (SodC) was unaffected (Fig. 1D). Recombinant ESAT6 expressed in *Lactococcus lactis*, as well as native ESAT6 isolated from the short-term culture filtrate of *M. tb* were tested for cytolysis of the less-sensitive cell type; both caused cytolysis of type 2 pneumocytes (Fig. S1).

To determine if the cytolytic ability of ESAT6 is retained when complexed to CFP10, heterodimers of ESAT6 and CFP10 were generated by mixing equimolar quantities in sodium phosphate buffer (Renshaw *et al.*, 2002). The formation of heterodimers was confirmed by an ELISA wherein the complexes were captured via anti-CFP10 IgG and detected with anti-ESAT6 antibodies (Fig. 2A). When the heterodimers were tested for their ability to lyse type 1 or type 2 pneumocytes, both cell types were lysed to the same extent as with free ESAT6. Thus, at ~10 μg ml^{-1} free and CFP10-complexed ESAT6, ~80% cytolysis of the type 1 and ~40% of the type 2 pneumocytes was observed at 72 h of incubation (Fig. 2B). These results demonstrate that ESAT6 retains its cytolytic competency when it is complexed to CFP10.

ESAT6 binds to type 1 and type 2 pneumocytes

To cause cytolysis, ESAT6 must bind to the membranes of the cells. Incubation of type 1 and type 2 cells with ESAT6 or CFP10 resulted in binding of only the former protein to both cell types (Fig. 3A and B). As implicated by the cytolysis experiments, ESAT6 binding to type 1 cells was greater than that to type 2 cells. Thus, while ESAT6 could be detected on the membranes of ~70% of the type 1 cells when added at 10 μg ml^{-1}, only ~20% of the type 2 cells showed binding at this concentration. Although at 20 μg ml^{-1}, the binding of ESAT6 to ~70% of the type 2 cells was obtained, the cytolysis of these cells did not increase (Fig. 1A). CFP10 did not show any significant binding to either cell type. Type 2 pneumocytes synthesize several ECM proteins and we have previously demonstrated the presence of laminin on the A549 cell membranes (Dunsmore and Rannels, 1996; Kinhikar *et al.*, 2006). Synthesis of ECM components by type 1 cells is not well-understood but since these cells are derived from type 2 pneumocytes, they were probed with anti-laminin antibodies to evaluate membrane laminin expression (Fig. 4A). Approximately 90% of both type 1 and type 2 pneumocytes exhibited the presence of laminin on their membranes; however, the mean fluorescence intensity on type 1 cells was significantly greater as compared with the type 2 cells, indicating that the amount of laminin per cell is higher in the former. These results were confirmed by evaluation of laminin in the cell membrane preparations of the two cell types (Fig. 4B). When the binding of ESAT6 to purified human laminin was tested, ESAT6 bound to immobilized laminin in a dose-dependent manner; no binding of ESAT6 was observed in BSA-coated wells (Fig. 4C). Moreover, when the binding of MS, a known laminin-binding adhesin, and SodC, which is not an adhesin was tested along with ESAT6, both MS and ESAT6 showed binding to laminin (Fig. 4D). Finally, anti-ESAT6 IgG demonstrated a dose-dependent (though partial) inhibition of binding of ESAT6 to immobilized laminin (Fig. 4E). Recombinant ESAT6 produced in *Lactococcus lactis* also bound to laminin in dose-dependent manner (Fig. S2). Together, these studies suggest that ESAT6 likely binds to the laminin in the membranes of type 1 and 2 pneumocytes, although the involvement of additional membrane components is not ruled out.

The M. tb *cell wall has minimal ESAT6*

While both ESAT6 and CFP10 were identified from the culture filtrates of *M. tb* (Berthet *et al.*, 1998), ESAT6 has also been reported to be a cell wall protein of *M. tb* (Pym *et al.*, 2002; Majlessi *et al.*, 2005). Considering the adhesive and lytic properties of ESAT6, we further investigated the surface localization of the protein. When the cell wall and SDS-extracted cell wall protein preparations of *M. tb* were probed for the presence of ESAT6 and CFP10, abundant CFP10 and minimal ESAT6 was detected in both preparations (Fig. 5A). Probing intact γ-irradiated bacteria for the presence of the 2 proteins on the bacterial cell surface also detected abundant CFP10 but minimal ESAT6 on the *M. tb* H_{37}Rv cell surface (Fig. 5B). As expected, neither protein was detected on intact γ-irradiated H_{37}Rv:Δ*RD1* or H_{37}Rv:Δ*esat6* bacteria (Fig. 5B). Examination of H_{37}Rv bacteria by immunoelectron microscopy confirmed the abundance of CFP10 and paucity of ESAT6 on the cell surface of *M. tb* grown *in vitro* (Fig. 5C–F).

Exogenously added ESAT6 associates with M. tb *cell wall*

Other Gram-positive bacteria express extracellular matrix (ECM) binding proteins that are shed into bacteriological media *in vitro* and can re-associate with the bacterial cell surface (Bergmann *et al.*, 2001; Chhatwal, 2002; Kinhikar *et al.*, 2006). It is possible that *in vivo*, most ESAT6 remains associated with the bacterial surface and confers the ability to be lytic to bacteria, while in the *in vitro* environment, it is shed into the culture filtrate. When the association of exogenously provided ESAT6 or CFP10 with intact γ-irradiated H_{37}Rv bacteria was tested, only the former protein associated with the bacterial surface (Fig. 6A). The association of ESAT6 to intact H_{37}Rv was observed both when anti-His and anti-ESAT6 antibodies were used for detection (Fig. 6A and B). In view of the abundance of CFP10 on the

M. tb cell surface and the ability of ESAT6 and CFP10 to form heterodimers, experiments to determine if the cell surface CFP10 is the receptor for association with exogenous ESAT6 were performed. Exogenously provided ESAT6 associated with intact H_{37}Rv:Δ*cfp10* or the H_{37}Rv:Δ*RD1* bacteria as well as it did with intact H_{37}Rv (Fig. 6B–D) ruling out the possibility of ESAT6 association with the bacterial surface via CFP10 or any of the proteins encoded by RD1.

Cell surface-associated ESAT6 is cytolytic

To determine if the cell surface-associated ESAT6 retains its cytolytic ability, γ-irradiated H_{37}Rv:Δ*RD1* bacteria were incubated with ESAT6, washed extensively and the ESAT6 bound to the bacteria quantified by ELISA to calculate the bacterial dose that would deliver sufficient ESAT6 to obtain cyotolysis of cells (Fig. S3). Bacterial concentrations calculated to carry ~2.5 μg ml^{-1}, ~1.25 and 0.625 μg ml^{-1} of ESAT6 were tested for cytolysis of the two cell types. Equal concentrations of γ-irradiated H_{37}Rv:Δ*RD1* bacteria were included as controls and no cytolysis of either cell type was observed at any of the bacterial concentrations of H_{37}Rv:Δ*RD1* (Fig. 6E). In contrast, dose-dependent cytolysis of type 1 cells was observed with H_{37}Rv:Δ*RD1* bacteria bearing ESAT6 (Fig. 6E). Thus, at the bacterial concentration calculated to present ~2.5 μg ml^{-1} of ESAT6, ~80% of the type 1 cells were lysed compared with the cells exposed to γ-irradiated H_{37}Rv:Δ*RD1*; at lower concentrations of ESAT6, the levels of cytolysis observed were lower (54% and 36% respectively). When the same bacterial suspensions were added to type 2 pneumocytes, ~8% cytolysis was obtained, only at the highest concentration of ESAT6 (Fig. 6E). As evident from Fig. 1A, ~2.5 μg ml^{-1} of ESAT6 would be expected to cause ~60% cytolysis to type 1 and ~20% to type 2 cells.

esat6 transcripts are increased in bacteria grown in type 1 and 2 cells

Previous studies have shown that passage of *M. tb* through macrophages or type 2 pneumocytes enhances the cytolytic phenotype (Bermudez *et al.*, 2002). In view of the cytolytic ability of ESAT6, experiments were performed to determine if *esat6* expression is upregulated in bacteria replicating in type 1 and 2 pneumocytes. Compared with *M. tb* growing in bacteriological media, transcripts of *esat6* in bacteria grown in type 1 cells were ~fourfold higher at 2 h (0 day) postinfection, and ~thirteen-fold higher by day 3. In bacteria growing in type 2 cells, the *esat6* transcripts were ~threefold and ~fivefold higher at the same time points (Fig. 7).

Discussion

The reduced cytolytic ability of BCG, H_{37}Rv:Δ*RD1*, H_{37}Rv:Δ*esat6* and H_{37}Rv:Δ*cfp10* bacteria, their reduced dissemination in animal models and the ability of ESAT6 to cause disruption of artificial planal membranes first implicated ESAT6 as a toxin of *M. tb* (Hsu *et al.*, 2003). The current studies demonstrate that ESAT6 is the mycobacterial toxin that can cause contact lysis of both type 1 and type 2 pneumocytes. The cytolytic ability is highly specific and under the same conditions, CFP10 which is coexpressed with ESAT6 and forms heterodimers with ESAT6, *M. tb* MS which has been demonstrated to be a cell wall and secreted laminin-binding protein, and SodC which is also a secreted protein but does not bind laminin, showed no cytolysis of either cell type (Wu *et al.*, 1998; Renshaw *et al.*, 2002; Kinhikar *et al.*, 2006). Since all four recombinant proteins tested carry a C-terminal His-tag and were expressed in *E. coli*, it is unlikely that either the His-tag or any contaminating host protein is responsible for the observed cytotolytic ability. Moreover, recombinant ESAT6 expressed in *Lactococcus lactis* and native ESAT6 isolated from the culture filtrate of *M. tb* also caused cytolysis of type 2 cells, the less sensitive cell type.

The binding of purified ESAT6 to the membranes of type 1 and type 2 pneumocytes both of which express laminin, the specific binding of ESAT6 to purified human laminin in ELISA,

and the blocking of the ESAT6–laminin interaction by anti-ESAT6 antibodies demonstrates that ESAT6 is a laminin-binding adhesin of *M. tb*. Anti-laminin antibodies were unable to block the ESAT6–laminin interaction (data not shown); possibly the commercial anti-laminin antibodies lack antibodies directed against the specific binding site(s) on laminin. Compared with type 2 cells, type 1 cells are significantly more sensitive to lysis by ESAT6; ~40% of type 1 cells were lysed at a concentration of 0.6 μg ml^{-1} of bacterium-associated protein (Fig. 6E). While the higher laminin content of the type 1 cell membranes and the correspondingly increased binding of ESAT6 would enhance their sensitivity for lysis, other factors are also involved since increased binding to type 2 pneumocytes at high concentrations of ESAT6 did not lead to a corresponding increase in cytolysis. Type 1 and type 2 cells may differ in the levels and isoforms of laminin in their membranes (Pierce *et al.*, 1998;DeBiase *et al.*, 2006) and ESAT6 binding to only particular laminin isoform(s) may result in cytolysis.

Considering the critical role of the RD1 region in the invasiveness of *M. tb in vivo* and the co-ordinated expression of *esat6* and *cfp10*, studies to understand the interaction between these proteins and with membranes have been performed (Hsu *et al.*, 2003). Structural studies determined that ESAT6 and CFP10 form a tight 1:1 complex and while the surface features of the complex were consistent with a function based on specific binding to one or more target proteins on host cells, a significant hydrophobic patch characteristic of a pore-forming protein was not identified (Renshaw *et al.*, 2002; 2005). Interestingly, while the initial studies with the artificial planal bilayers showed that ESAT6 alone or ESAT6–CFP10 complexes cause disruption of the bilayers, subsequent studies suggested that the complexes did not bind to liposomes while free ESAT6 could bind and cause their lysis (Hsu *et al.*, 2003; de Jonge *et al.*, 2007). Recently, ESAT6 alone, or in combination with CFP10, has been demonstrated to cause dose-dependent lysis of red blood cells and macrophages, although this required high concentrations of ESAT6 (30 μg ml^{-1}) for complete lysis (Smith *et al.*, 2008). Osmoprotection studies indicate that the lysis is due to pore-formation in the membranes and the pore-size caused by bacterium-associated ESAT6 is larger than the pores caused by purified recombinant ESAT6, suggesting that the bacteria-associated ESAT6 differs in multimerization and/or membrane insertion from free ESAT6 (Smith *et al.*, 2008). Our results with pneumocytes concur with those observed with red blood cells and macrophages in that the cytolytic ability of ESAT6 is retained when it is complexed with CFP10, or is present on the cell surface of intact bacteria. Interestingly, compared with red blood cells, almost complete destruction of the type 1 monolayers was observed at much lower ESAT6 concentrations (6–10 μg ml^{-1}; Fig. 1A) and when ESAT6 was associated with the bacterial surface, ~80% of the type1 cells were lysed at 2.5 μg ml^{-1} of ESAT6 (Fig. 6E). Together, these results suggest that ESAT6 possesses both a laminin-binding domain and a pore-forming domain, and anchoring on the pneumocyte cell membrane via binding to laminin facilitates achievement of high local concentrations of ESAT6, increasing the efficiency of pore formation, and thus, lysis, by bacteria expressing ESAT6 on their surface. Our preliminary experiments using ESAT6 peptides to identify the laminin-binding and/or the lytic domains were unsuccessful suggesting that conformational constraints may be involved in both binding and lytic functions.

In view of its adhesive and lytic functions, and the attenuated dissemination of BCG, H_{37}Rv:Δ*RD1*, H_{37}Rv:Δ*esat6* and H_{37}Rv:Δ*cfp10* mutants, we expected ESAT6 to be localized to the bacterial cell wall. However, while abundant CFP10 was confirmed to be present on the bacterial surface, neither the ELISA with cell wall protein preparations, nor the ELISA or immunoelectron microscopy with intact bacteria demonstrated the anticipated localization. The association of exogenous ESAT6 with the cell wall, and the retaining of the lytic function by the cell wall associated ESAT6 suggests that although under *in vitro* conditions ESAT6 is shed into bacteriological media, *in vivo* ESAT6 may be retained on the bacterial surface (Pym *et al.*, 2002). Differences in subcellular localization of *M. smegmatis* ESAT6 and PirG protein in bacteria grown in different media have been reported (Kocincova *et al.*, 2004; Converse and

Cox, 2005). Considering that exogenously provided ESAT6 associates equally well with the bacteria lacking CFP10 on the cell wall, it is possible that the association of ESAT6 with the cell surface is sensitive to pH/charge/ionic changes in the environment, as also reported for some other adhesins (D'Costa *et al*., 2000; Antikainen *et al*., 2007); however, the involvement of a non-RD1-related receptor cannot be ruled out. Our results showing upregulation of *esat6* transcripts in bacteria replicating in pneumocytes indicate that its expression likely increases in these bacteria. Although recent studies suggested that the function of ESAT6 is controlled by regulation of its secretion, no studies have been performed to directly correlate upregulation of transcripts with increased secretion (Frigui *et al*., 2008). However, expression of ESAT6 by intracellularly replicating bacteria in the lungs of mice infected with BCG:*RD1* (Majlessi *et al*., 2005) and upregulation of *esat6* transcripts in bacteria recovered from infected mice (Rogerson *et al.*, 2006) has been reported.

Earlier studies demonstrated that *M. tb* infection causes apoptosis in human macrophages and necrosis in alveolar epithelial cells *in vitro* (Danelishvili *et al.*, 2003). *M. tb* lacking the *cfp10esat6* operon are attenuated for cell lysis and tissue invasiveness in mice (Hsu *et al.*, 2003). Progressive infection with mycobacteria lacking the RD1 region (BCG or *M. tb* H_{37}Rv*:*Δ*RD1*) fails to cause necrosis and destruction of the lung parenchyma in mice lacking γ-interferon (Junqueira-Kipnis *et al*., 2006). Moreover, both BCG and H_{37}Rv*:*Δ*RD1* show delayed dissemination from the lungs to the spleen (Converse and Cox, 2005). While ESAT6 consistently caused lysis of both type 1 and 2 pneumocytes, the cells failed to show the characteristic ladder pattern of apoptotic DNA, indicating that the ESAT6-mediated lysis is caused by necrosis (data not shown). Our studies with pneumocytes implicate ESAT6 as the bacterial toxin that is responsible for the pulmonary necrosis observed *in vivo* although the confirmation of this will be possible only when the precise binding sites on ESAT6 and/or laminin are identified and the interaction between the two can be interrupted. This ability of the same molecule to lyse cells via different apoptotic pathways and also necrosis has also been reported for pneumolysin (PLY) of *Streptococcus pneumoniae* (Garcia-Suarez Mdel *et al.*, 2007).

The alveolar wall comprises primarily type 1 and type 2 pneumocytes that cover the epithelial basement membrane, which in turn is fused to the basement membrane of the capillary endothelium (Dunsmore and Rannels, 1996). This basement membrane, with pneumocytes on one side and endothelial cells on the other, is composed primarily of laminin and collagen IV (Dunsmore and Rannels, 1996). Although in tissue culture grown cells, laminin is distributed over the cell membranes, *in vivo*, laminin is concentrated primarily to the basolateral surface of the epithelial cells where they make contact with the basement membranes (Dunsmore and Rannels, 1996). The ability of ESAT6 to bind to laminin, to lyse the cell membranes of both type 1 and 2 pneumocytes, to retain its lytic ability when associated with the bacterial surface and the rapid upregulation of the *esat6* transcripts in bacteria growing intracellularly together suggest a scenario in which *M. tb* that has invaded pneumocytes may enhance their invasive phenotype by upregulating the expression of ESAT6, thus increasing their ability to bind to the basolateral laminin-expressing surface of the cells and damage the cells and the basement membrane to directly disseminate through the alveolar barrier. Damage to even a small number of cells would be sufficient to enable dissemination. This scenario is supported by earlier studies demonstrating that *M. tb* that have replicated in type 2 pneumocytes acquire a highly invasive phenotype for invasion of endothelial cells and that endothelial cells also express laminin (Bosman and Stamenkovic, 2003). Interestingly, BCG has been demonstrated to be attenuated for cell-free translocation across the bilayer model of the alveolar wall (Bermudez *et al.*, 2002). The damage to the alveolar epithelium and cytokine release by pneumocytes could elicit enhanced migration of inflammatory cells to the alveoli, further encouraging dissemination via infected phagocytic cells as well as attracting cells that contribute to granuloma formation (Lin *et al.*, 1998). It could also provide an opportunity for the

dissemination of free bacteria via the circulation, although whether this occurs in tuberculosis has not been investigated.

Infection of epithelial cells and dissemination via adhesion, invasion and damage to the epithelial cells of the mucosal barriers is a common theme in infections with other pathogens that cause pulmonary diseases. Thus, during the initial phases of infection, *S. pneumoniae* expresses a PLY, a toxin that is cytolytic for type 1 and type 2 pneumocytes and endothelial cells (Rubins *et al.*, 1993), and can disrupt the alveolar–capillary boundary enabling the penetration of the bacteria from the alveoli into the bloodstream (Rubins and Janoff, 1998). Interestingly, type 1 pneumocytes are significantly more sensitive to cytotoxicity by PLY as compared with type 2 cells and PLY has been implicated as an adhesin for respiratory epithelial cells (Rubins and Janoff, 1998; Rubins *et al.*, 1998). *Pneumocystis carini* also binds preferentially to type 1 penumocytes and adhesion and damage to these cells results in breaching the alveolar epithelium and allows enhanced dissemination to the other organs, including the lymph nodes, spleen, bone marrow and liver (Nakamura and Wada, 1998; Kaneshiro, 2001). The high sensitivity of type 1 pneumocytes to ESAT6-mediated cytolysis and the greater upregulation of the *esat6* transcripts in bacteria replicating in these cells emphasize the potential importance of the *M. tb*–type 1 pneumocyte interaction for acquiring a highly invasive phenotype by *in vivo M. tb* that enables the establishment of infection by the few bacteria that are inhaled.

Dissemination of *M. tb* from the lungs to extrapulmonary sites occurs early during the infection process, before the cellular immune responses that control the infection are elicited (Chackerian *et al.*, 2002; McMurray, 2003). The presence of memory ESAT6-specific T cells that express IFN-γ in the healthy latently infected subjects indicates that this protein is expressed by the *M. tb* soon after infection. Further studies on the role of ESAT6 as a mycobacterial adhesin and toxin are required for the development of strategies that can prevent the invasion and dissemination of bacteria that is vital for establishing infection.

Experimental procedures

Cell lines

The human type 1 alveolar pneumocyte-like cell line (WI26; WI-26 VA4; ATCC CCL95.1) and type 2 alveolar pneumocyte cell line (A549; ATCC CCL185) were procured from the American Type Culture Collection, Rockville, MD, USA, grown in appropriate media, and the cells aliquoted and frozen in liquid nitrogen. The type 1 cells were propagated in RPMI 1640 supplemented with 10% de-complemented FBS (Hyclone, Logan, UT), 1% L-glutamine (Lonza, MD), 1% non-essential amino acids (Sigma), 1% HEPES (Sigma) and 1% sodium pyruvate (Sigma); the type 2 cells in RPMI 1640 supplemented with 7.5% FBS, 1% L-glutamine and 1% non-essential amino acids.

Mycobacterial preparations

Mycobacterium tuberculosis H_{37}Rv, H_{37}Rv:Δ*RD1*, H_{37}Rv:Δ*esat6* and H_{37}Rv:Δ*cfp10* were grown in roller bottles with glycerol-alanine-salt (GAS) media supplemented with 0.05% tween 80. After 14 days, the bacteria were pelleted, washed once with chilled PBS containing 0.05% tween 80 and twice with chilled deionized autoclaved water. Bacteria were inactivated by exposing the wet pellet to 2.4 mrads of γ-irradiation using a ^{137}Cs source. *M. tb* subcellular fractions (total cell wall and SDS-extracted cell wall proteins) and His-tagged ESAT6 (*Rv3875*), malate synthase (*Rv 1837c*), CFP10 (*Rv3874*) and superoxide dismutase C (*Rv0432*) purified by Ni-iminodiacetic acid-affinity chromatography were obtained from the NIH/NIAID TB Research Materials and Vaccine Testing Contract, Colorado State University, Fort Collins (http://www.cvmbs.colostate.edu/mip/tb/sop.htm). Recombinant ESAT6

(ESAT6) expressed in *Lactococcus lactis* and native ESAT6 isolated from culture filtrate of H_{37}Rv were obtained from SSI, Denmark.

Reagents for ELISA and FACS studies

Alkaline phosphatase (AP)-conjugated goat anti-rabbit IgG and AP-rabbit anti-mouse IgG were from Sigma Chemical, St Louis, MO, USA. FITC-goat anti-rabbit IgG and FITC-rabbit anti-mouse IgG were from Zymed Laboratories, San Francisco, CA, USA. The ELISA amplification system was from Invitrogen Life Technologies Corporation, Carlsbad, CA, USA. Polyclonal anti-*M. tb* ESAT6 and CFP10 Abs were obtained by immunization of New Zealand white rabbits with purified ESAT6 or CFP10 (in Incomplete Freund's Adjuvant, Sigma). Serum IgG from pre- and post-immunization sera was affinity-purified (protein A sepharose 4B; Amersham Biosciences, Uppsala, Sweden). Polyclonal anti-ESAT6 antibodies were also obtained by immunization of BALB/c mice. Anti-His antibodies were obtained from Qiagen, CA, USA. Polyclonal anti-laminin antibodies were obtained from Chemicon, CA, USA; these antibodies react with multiple isoforms of laminin.

Evaluation of cytolytic potential of ESAT6 and CFP10

Aliquots of frozen type 1 and type 2 cells were thawed and ~1×10^6 cells allowed to form monolayers in the T-75 flasks (5–6 days for type 1 and 4–5 days for type 2 pneumocytes). On the day of the experiment, the cells were detached with 10 mM EDTA, washed with medium and 50 μl of 4×10^5 cells ml^{-1} suspension dispensed in each well of 96-well flat-bottom tissue culture plate (Corning). To monitor the cytolytic potential of *M. tb* proteins, 50 μl of different concentrations of proteins (3–15 μg ml^{-1}) was added in six wells, and the plates incubated for 24, 48 and 72 h at 37°C in 5% CO_2. Cells exposed to culture medium alone were included as controls. At the end of incubation the viability of cells was determined by MTT assay/ microscopy visualization.

MTT assay

The MTT assay was performed using 3-(4,5-dimethylthiazol-2-yl)-2,5-diphenyltetrazolium bromide as per the manufacturer's instructions (Invitrogen). The culture supernatant from each well was removed and 110 μl of 1.2 mM MTT solution prepared in BD cell MAb medium (without phenol red; Becton and Dickinson and company, MD) was added. The plate was incubated for 4 h at 37°C in 5% CO_2, centrifuged at 400 *g* for 10 min at room temperature and supernatants from the wells were discarded. The pelleted insoluble formazan was dissolved in 50 μl of dimethyl sulphoxide (DMSO; Sigma) and the colour read at 530 nm. Per cent cytolysis was calculated by using the formula: (Mean OD_{530} of control wells – Mean OD_{530} of test wells)/(Mean OD_{530} of control wells) × 100.

Cytolysis by ESAT6:CFP10 complex

Confirmation of complex formation—Earlier studies have reported that mixing ESAT6 and CFP10 in equimolar ratios results in the formation of complexes (Renshaw *et al.*, 2002). To confirm that mixing actually resulted in complex formation, a sandwich ELISAwas designed. Wells of an ELISAplate were coated with rabbit anti-CFP10 IgG at 5 μg ml^{-1} for 2 h at 37°C followed by overnight (ON) at 4°C, washed with PBS, and blocked with 1% BSA for 2 h at 37°C. A mixture of ESAT6 plus CFP10 (at 1:1 molar ratio, 10 μg ml^{-1} and 16.6 μg ml^{-1} final concentration respectively) was incubated for 30 min at 37°C and 50 μl of 1:10, 1:50, 1:100 and 1:200 dilutions of the mixture (containing 1, 0.2, 0.1 and 0.05 μg ml^{-1} ESAT6 respectively), and equal concentrations of ESAT6 alone, were added to the anti-CFP10- coated and blocked wells in triplicates. The plate was incubated for 2 h at 37°C, washed with PBST-0.05% (PBS containing 0.05% tween 20) and the captured ESAT6 detected with mouse

anti-ESAT6 serum (1:10 000) followed by AP-conjugated anti-mouse IgG (1:5000) and substrate.

Determination of the cytolytic potential of the ESAT6:CFP10 complex—ESAT6 was allowed to form complex with CFP10 by mixing in 1:1 molar ratio and incubating for 30 min at 37°C. The protein-mixture as well as ESAT6 alone was then tested in cytolytic assay as described above. Briefly, cells from WI26 and A549 monolayers were harvested using 10 mM EDTA, washed with RPMI 1640 and 50 μl of 4×10^5 cells ml^{-1} suspension made in culture medium was dispensed in each well of 96 well flat-bottom tissue culture plates. ESAT6 alone and ESAT6–CFP10 mixture was adjusted to contain 20 μg ml^{-1} of ESAT6. Fifty μl of the above protein solutions were added to cells in 6 wells each so that the final concentration of ESAT6 in each well was 10 μg ml^{-1}. The cells were incubated for 72 h at 37°C in 5% CO2. At the end of incubation, MTT assay was carried out. Cells alone (without protein) were used as control to calculate the percentage cytolysis.

Evaluation of interaction of ESAT6 and CFP10 with pulmonary epithelial cells

Binding of* M. tb *proteins to alveolar epithelial cells—The binding of *M. tb* proteins to alveolar epithelial cells was determined as described earlier (Kinhikar *et al.*, 2006). Briefly, cells harvested from monolayers of WI26 and A549 cells were washed with RPMI 1640 and 5×10^5 cells (in triplicates) were suspended in 200 μl PBS containing 10 or 20 μg ml^{-1} of *M. tb* ESAT6 or CFP10. After 30 min of incubation at 37°C, the cells were washed with PBS/0.1% BSA, and suspended in 200 μl of PBS/0.1% BSA containing the anti-His IgG (1:500) for 45 min at 4°C. After washing, the cells were exposed to FITC-rabbit anti-mouse IgG (1:250) for 20 min at 4°C, washed and fixed with 4% formaldehyde (Sigma). The cell-associated fluorescence (% FITC labelled cells) was quantified on a FACSCalibur flow cytometer (BD Immunocytochemistry Systems, San Jose, CA). Cells exposed to anti-His IgG and FITC-conjugated rabbit anti-mouse IgG (no ESAT6) were used to determine non-specific binding of the antibodies.

Presence of laminin on the membranes of alveolar epithelial cells—Cells were harvested from monolayers, and 5×10^5 cells were pelleted by centrifugation at 400 *g*. The cell-pellet was suspended in 200 μl of rabbit anti-laminin antibodies (1:200) or normal rabbit antibodies for 30 min at 4°C, after which the cells were washed and exposed to FITC-conjugated goat anti-rabbit IgG (1:250) for 20 min at 4°C, washed again and fixed with 4% formaldehyde. The cell-associated fluorescence (% FITC labelled cells) was quantified on a flow cytometer and was also examined under fluorescent microscope with 100× magnification. The mean fluorescence intensity associated with the stained cells was calculated using FlowJo software (Tree star, Ashland, OR).

The presence of laminin in the membrane preparations of the two cell types was also determined by ELISA. To prepare the membrane fractions, cells were harvested from monolayers as described, washed thrice with PBS and suspended at 5×10^8 cells ml^{-1} in ice-cold Dounce buffer (20 mM Hepes buffer, 1 mM EGTA, pH 7.6) with 0.25% protease inhibitor cocktail (Sigma). The cell suspension was added into a pre-chilled, tight-fitting Dounce homogenizer, subjected to 30 strokes and centrifuged at 800 *g*, 10 min at 4°C. The supernatant was transferred into a polycarbonate ultracentrifuge tube (Beckman Instruments, Palo Alto, CA) and centrifuged (45 000 *g*; Optima Max Ultracentrifuge, rotor TLA 110, Beckman Instruments) for 10 min at 4°C. The membrane pellet was washed with Dounce buffer, resuspended in same buffer containing protease inhibitors, protein content was estimated using BCA kit (Pierce) and stored at –80°C until use.

Wells of an ELISA plate were coated with various concentrations (1–5 μg ml^{-1}) of the cell-membrane for 2 h at 37°C followed by overnight (ON) at 4°C. The wells were washed with PBS, blocked with 1% BSA, washed again with PBST-0.05% and 50 μl of rabbit anti-laminin IgG (1:5000) was added to each well; wells exposed to IgG from normal rabbit serum were included as controls. The bound anti-laminin antibodies were detected with AP-conjugated goat anti-rabbit IgG (1:4000), followed by substrate. O.D. was determined at 490 nm.

Binding of M. tb *ESAT6 to purified laminin*

The binding of ESAT6 to purified laminin was examined by ELISA. Wells of an ELISA plate were coated with 50 μl of laminin-1 (from human placenta; Sigma) suspended in PBS at 1 μg ml^{-1}, blocked with 1% BSA-PBS and 50 μl of different concentrations (2.5–7.5 μg ml^{-1}) of purified ESAT6, were added. Wells coated with similar concentrations of BSA were used as controls. The ESAT6 bound to the immobilized laminin or BSA was detected by use of rabbit anti-ESAT6 IgG (0.3 μg ml^{-1}) and AP-conjugated goat anti-rabbit IgG (1:4000, Sigma).

To further confirm the specificity of binding of ESAT6 to laminin, wells of an ELISA plate were coated with laminin and blocked as above, and different concentrations (2.5–7.5 μg ml^{-1}) of purified ESAT6, MS and SodC were added. The binding of the 3 recombinant proteins with laminin was detected with anti-His mAbs (1; 2000) followed by AP-conjugated anti-mouse IgG (1:2000).

The ability of anti-ESAT6 antibodies to inhibit the laminin-ESAT6 binding was also evaluated. ELISA plates were coated with laminin and blocked as above. Separately, 100 μl of ESAT6 (10 μg ml^{-1}) was mixed with 100 mls of rabbit anti-ESAT-6 IgG or pre-immune IgG (1 μg ml^{-1}) at dilutions of 1:250 or 1:500 over night at 4°C. Fifty μls of the ESAT6-IgG mixture was added to the laminin coated wells (in triplicates) and incubated for 1 h at 37°C. The laminin bound ESAT-6 was detected with anti-His mAbs (1:2000) followed by AP-conjugated anti-mouse IgG (1:2000). Per cent inhibition was calculated by considering the binding of ESAT6 alone (5 μg ml^{-1}) as 100% binding.

Localization of M. tb *ESAT6 and CFP10*

Mycobacterium tuberculosis $H_{37}Rv$ CW and SDS-CW preparations (2 μg ml^{-1} in PBS, pH 7.0) were coated in ELISA plates (50 μl $well^{-1}$) for 2 h at 37°C followed by ON at 4°C, washed with PBS, blocked with BSA-PBS (1% BSA), washed with PBST-0.05% and exposed to rabbit anti-ESAT6 or anti-CFP10 IgG or pre-immune IgG (~0.3 μg ml^{-1}) for 1.5 h at 37°C. The bound antibodies were detected with AP-conjugated goat anti-rabbit IgG (1:4000). ΔOD (OD_{490} in wells probed with anti-ESAT6/CFP10 IgG – OD_{490} in wells exposed to pre-immune IgG) was calculated.

To confirm the presence of ESAT6 or CFP10 on the surface of bacterial cells, γ-irradiated *M. tb* $H_{37}Rv$ or $H_{37}Rv$*:*Δ*esat6* or *M. tb* $H_{37}Rv$*:*Δ*RD1* was suspended at 3×10^8 bacilli ml^{-1} (1 McFarland) in PBS and serial dilutions of the bacteria were transferred to ELISA plate (50 μl $well^{-1}$) in triplicates (37°C for 2 h followed by ON at 4°C) (Kinhikar *et al.*, 2006). The wells were washed with PBS, blocked with 1% BSA-PBS, washed with PBST-0.05%, and exposed to rabbit anti-ESAT6 IgG or anti-CFP10 IgG or pre-immune IgG (50 μl $well^{-1}$; ~0.3 μg ml^{-1}) for 1.5 h at 37°C. Delta OD was calculated as described.

To further confirm the presence of ESAT6 or CFP10 on the surface of bacterial cells, γ-irradiated *M. tb* $H_{37}Rv$ bacilli were fixed with 3% paraformaldehyde in 0.1 M sodium cacodylate buffer containing 0.1% glutaraldehyde and 4% sucrose, washed and dehydrated before being embedded in Lowicryl K4M (Polysciences, Warrington, PA, USA) and polymerized under UV light (360 nm) at –35°C. Ultrathin sections (70 nm) were incubated

with anti-ESAT6 IgG or anti-CFP10 IgG or pre-immune IgG (1:25) at 4°C ON, exposed to gold conjugated protein A (Cell Microscopy Center, CX Utrecht, Netherlands), stained with uranyl acetate and lead citrate and examined under Philips CM-12 electron microscope at NYU Image Core Facility.

Association of exogenous ESAT6 with bacterial cell surface and the cytolytic potential of bacterium-associated ESAT6

Serial dilutions of γ-irradiated *M. tb* H_{37}Rv suspended at 3×10^8 bacilli ml^{-1} (1 McFarland) were plated in wells of an ELISA plate (50 μl $well^{-1}$) and incubated at 4°C overnight. The wells were blocked with BSA and 50 μl of ESAT6 or CFP10 suspended at 2 μg ml^{-1} added to the wells. The wells were washed after 90 min, and the *M. tb*-bound recombinant proteins were detected by anti-His mAbs (1:2000) and AP-conjugated rabbit anti-mouse IgG (1:5000).

Association of ESAT6 to γ-irradiated *M. tb* H_{37}Rv, H_{37}Rv:Δ*cfp10* or *M. tb* H_{37}Rv:Δ*RD1* was also determined by using rabbit anti-ESAT6 IgG. Briefly, after plating the serial dilutions of above bacteria, the blocked wells were exposed for 90 min to 50 μl of ESAT6 suspended at 2 μg ml^{-1} and the bound protein was determined by using rabbit anti-ESAT6 IgG (0.3 μg ml^{-1}) and AP-Goat anti-rabbit IgG (1:4000).

To determine if the bacterium-associated ESAT6 is cytotoxic, γ-irradiated H_{37}Rv:Δ*RD1* cells (9×10^9 bacilli) were incubated with or without (control) 450 μg of ESAT6 in a total volume of 450 μl (PBS) at 37°C for 2 h followed by ON at 4°C. The bacteria were washed three times with RPMI and suspended in 450 μl of medium and 30 μl of this bacterial suspension was removed to quantify the bacteria-associated ESAT6. The bacteria in the 30 μl aliquot were washed twice with PBS-0.05% tween 80 and once with PBS to remove any unbound ESAT6 and suspended at 3×10^8 bacilli ml^{-1} (1 McFarland; MF) in PBS. Fifty microlitres of this suspension was placed in ELISA plate in triplicate. Ten double dilutions of purified ESAT6 suspended at 3 μg ml^{-1} were also plated (in triplicate) in the wells of same ELISA plate. After ON incubation at 4°C, the wells were blocked with 1% BSA, and ESAT6 detected using rabbit anti-ESAT6 IgG (0.3 μg ml^{-1}) and AP-Goat antirabbit (1:4000) as described above. The OD_{490} obtained with the bacteria in the ELISA was plotted on the standard curve obtained with purified ESAT6 to quantify the bacterial surface ESAT6; 50 μl of 3×10^8 bacilli ml^{-1} (1MF) carried 0.055 μg ml^{-1} ESAT6 (Fig. S3). The remaining 8.4×10^9 bacilli (in 420 μl of bacterial suspension) were suspended in a final volume of 650 μl, so that 50 μl of this bacterial suspension would carry ~2.5 μg ml^{-1} ESAT6.

WI26 and A549 cells were harvested from monolayers with 10 mM EDTA, washed with RPMI 1640 and 2×10^4 cells suspended in RPMI dispensed in each well of 96-well flat-bottom tissue culture plate. Fifty microlitres per well of the H_{37}Rv:Δ*RD1* bacterial suspension (with ESAT6 equivalent of ~2.5, 1.25 and 0.625 μg ml^{-1}) was added to wells containing 50 μl of cells (in triplicate) and the plate was incubated for 72 h at 37°C in 5% CO_2. After incubation, MTT assay was carried out as described above. Per cent cytolysis was calculated by using the formula: (Mean OD_{530} in wells containing cells incubated with bacteria alone – Mean OD_{530} of wells containing cells exposed to bacteria-ESAT6)/(Mean OD_{530} of wells containing cells incubated with bacteria) × 100.

Quantitative real-time RT-PCR (qRT-PCR)

Monolayers of WI26 and A549 cells in tissue culture flasks (225 cm^2 Corning) were infected with single cell suspension of log phase *M. tb* H_{37}Rv grown in Middlebrook 7H9 broth at multiplicities of infection of 1:10 (I0 bacteria/cell) and 1:5 for 2 h at 37°C. The infected cells were washed with warm RPMI and maintained in the RPMI containing 1% FBS, 2 mM L-glutamine and 1% non-essential amino acid for 5 days at 37°C. At each time points [2 h (0

day), 3, and 5 days], the infected cells were lysed with GTC solution (4 M guanidinium thiocynate, 0.5% sodium N-lauryl sarcosine, 25 mM tri-sodium citrate, 0.1 M 2-mercaptoethanol, 0.5% Tween 80, pH 7.0) and centrifuged at 5000 *g* for 20 min at 4°C to pellet bacteria (Butcher *et al*., 1999). The pellets were washed in GTC solution and resuspended in TRI reagent containing polyacrylamide carrier (Molecular Research Center, Cincinnati, OH, USA). Total RNA was extracted by using the protocol described previously (Fontan *et al.*, 2008). RNA from log phase culture of *M. tb* H_{37}Rv grown in 7H9 medium was also extracted.

For qRT-PCR, the total RNA preparations were subjected to reverse transcriptase (RT) reaction to synthesize first-strand cDNA using Superscript II RNase H^- reverse transcriptase (Invitrogen Corporation, Carlsbad, CA, USA) according to manufacturer's protocol. For each RNA sample, a reaction without RT was also performed as a negative control. Using cDNA as template, PCR reaction was performed in 20 μl reaction volume containing 1× iQ SYBER Green supermix (Bio-Rad, CA) and 0.5 μM of gene specific primers (Table S1) on MiniOpticon detection system as per the manufacturer's protocol (Bio-Rad). The specificity of the RT-PCR products obtained with RNA from *M. tb* grown in Middlebrook 7H9 media and the host cells with each primer pair used was initially confirmed by DNA sequencing and by melting curve analysis in the subsequent assays. For calculation of cDNA copies, a standard curve was generated for each gene using a serial dilution of *M. tb* genomic DNA and respective specific primers. The copies of 16S rRNA was used to normalize the transcript levels of the *esat6* and 23S rRNA (included as control). The fold change in expression of *esat6* and 23S rRNA was determined by calculating the ratio of normalized copies of these genes in bacteria obtained from WI26 or A549 cells to 7H9 broth-grown bacteria.

Statistical analysis

The unpaired *t*-test and two-way ANOVA were used for analysis of statistical significance with GraphPad Prism version 5 software (GraphPad Software, San Diego, CA, USA). A *P*-value of < 0.05 was considered as statistically significant.

Supplementary Material

Refer to Web version on PubMed Central for supplementary material.

Acknowledgments

We would like to thank Catarina Hioe for the FlowJo analysis, Diana Virland for running samples on FACS and Flavia Camacho for the figures. A.K. is supported by Research Enhancement Award Program (REAP) funded by the Department of Veterans Affairs. These studies were also supported by a V. A. Merit Review Award and National Institutes of Health (NIH) grant R01 AI-056257, and by NIH/NIAID contract NO1-AI-75320 entitled 'TB Research Materials and Vaccine Testing'. The authors have no conflicting financial interests.

References

Antikainen J, Kuparinen V, Lahteenmaki K, Korhonen TK. Ph-dependent association of enolase and glyceraldehyde-3-phosphate dehydrogenase of *Lactobacillus crispatus* with the cell wall and lipoteichoic acids. J Bacteriol 2007;189:4539–4543. [PubMed: 17449624]

Bergmann S, Rohde M, Chhatwal GS, Hammerschmidt S. Alpha-enolase of *Streptococcus pneumoniae* is a plasmin (ogen)-binding protein displayed on the bacterial cell surface. Mol Microbiol 2001;40:1273–1287. [PubMed: 11442827]

Bermudez LE, Sangari FJ, Kolonoski P, Petrofsky M, Goodman J. The efficiency of translocation of *Mycobacterium tuberculosis* across a bilayer of epithelial and endothelial cells as a model of the alveolar wall is a consequence of transport within mononuclear phagocytes and invasion of alveolar epithelial cells. Infect Immun 2002;70:140–146. [PubMed: 11748175]

Berthet FX, Rasmussen PB, Rosenkrands I, Andersen P, Gicquel B. A *Mycobacterium tuberculosis* operon encoding ESAT-6 and a novel low-molecular-mass culture filtrate protein (CFP-10). Microbiology 1998;144:3195–3203. [PubMed: 9846755]

Birkness KA, Deslauriers M, Bartlett JH, White EH, King CH, Quinn FD. An *in vitro* tissue culture bilayer model to examine early events in *Mycobacterium tuberculosis* infection. Infect Immun 1999;67:653–658. [PubMed: 9916072]

Bosman FT, Stamenkovic I. Functional structure and composition of the extracellular matrix. J Pathol 2003;200:423–428. [PubMed: 12845610]

Butcher PD, Mangan JA, Monahan IM. Intracellular gene expression – analysis of RNA from mycobacteria in macrophages using RT-PCR. Methods Mol Biol 1999;101:285–306. [PubMed: 9921487]

Chackerian AA, Alt JM, Perera TV, Dascher CC, Behar SM. Dissemination of *Mycobacterium tuberculosis* is influenced by host factors and precedes the initiation of T-cell immunity. Infect Immun 2002;70:4501–4509. [PubMed: 12117962]

Chhatwal GS. Anchorless adhesins and invasins of Gram-positive bacteria: a new class of virulence factors. Trends Microbiol 2002;10:205–208. [PubMed: 11973142]

Converse SE, Cox JS. A protein secretion pathway critical for *Mycobacterium tuberculosis* virulence is conserved and functional in *Mycobacterium smegmatis*. J Bacteriol 2005;187:1238–1245. [PubMed: 15687187]

D'Costa SS, Romer TG, Boyle MD. Analysis of expression of a cytosolic enzyme on the surface of *Streptococcus pyogenes.* Biochem Biophys Res Commun 2000;278:826–832. [PubMed: 11095992]

Danelishvili L, McGarvey J, Li YJ, Bermudez LE. *Mycobacterium tuberculosis* infection causes different levels of apoptosis and necrosis in human macrophages and alveolar epithelial cells. Cell Microbiol 2003;5:649–660. [PubMed: 12925134]

DeBiase PJ, Lane K, Budinger S, Ridge K, Wilson M, Jones JC. Laminin-311 (Laminin-6) fiber assembly by type I-like alveolar cells. J Histochem Cytochem 2006;54:665–672. [PubMed: 16714422]

Derrick SC, Morris SL. The ESAT6 protein of *Mycobacterium tuberculosis* induces apoptosis of macrophages by activating caspase expression. Cell Microbiol 2007;9:1547–1555. [PubMed: 17298391]

Dobos KM, Spotts EA, Quinn FD, King CH. Necrosis of lung epithelial cells during infection with *Mycobacterium tuberculosis* is preceded by cell permeation. Infect Immun 2000;68:6300–6310. [PubMed: 11035739]

Dunsmore SE, Rannels DE. Extracellular matrix biology in the lung. Am J Physiol 1996;270:L3–L27. [PubMed: 8772523]

Fontan P, Aris V, Ghanny S, Soteropoulos P, Smith I. Global transcriptional profile of *Mycobacterium tuberculosis* during THP-1 human macrophage infection. Infect Immun 2008;76:717–725. [PubMed: 18070897]

Frigui W, Bottai D, Majlessi L, Monot M, Josselin E, Brodin P, et al. Control of *M. tuberculosis* ESAT-6 secretion and specific T cell recognition by PhoP. PLoS Pathog 2008;4:e33. [PubMed: 18282096]

Galvan EM, Chen H, Schifferli DM. The Psa fimbriae of *Yersinia pestis* interact with phosphatidylcholine on alveolar epithelial cells and pulmonary surfactant. Infect Immun 2007;75:1272–1279. [PubMed: 17178780]

Garcia-Suarez Mdel M, Florez N, Astudillo A, Vazquez F, Villaverde R, Fabrizio K, et al. The role of pneumolysin in mediating lung damage in a lethal pneumococcal pneumonia murine model. Respir Res 2007;8:3. [PubMed: 17257395]

Geijtenbeek TB, Van Vliet SJ, Koppel EA, Sanchez-Hernandez M, Vandenbroucke-Grauls CM, Appelmelk B, Van Kooyk Y. Mycobacteria target DC-SIGN to suppress dendritic cell function. J Exp Med 2003;197:7–17. [PubMed: 12515809]

Guinn KM, Hickey MJ, Mathur SK, Zakel KL, Grotzke JE, Lewinsohn DM, et al. Individual RD1-region genes are required for export of ESAT-6/CFP-10 and for virulence of *Mycobacterium tuberculosis*. Mol Microbiol 2004;51:359–370. [PubMed: 14756778]

Harb OS, Abu Kwaik Y. Essential role for the *Legionella pneumophila* rep helicase homologue in intracellular infection of mammalian cells. Infect Immun 2000;68:6970–6978. [PubMed: 11083821]

Hsu TSM, Hingley-Wilson B, Chen M, Chen AZ, Dai PM, Morin CB, et al. The primary mechanism of attenuation of bacillus Calmette-Guerin is a loss of secreted lytic function required for invasion of lung interstitial tissue. Proc Natl Acad Sci USA 2003;100:12420–12425. [PubMed: 14557547]

Humphreys IR, Stewart GR, Turner DJ, Patel J, Karamanou D, Snelgrove RJ, Young DB. A role for dendritic cells in the dissemination of mycobacterial infection. Microbes Infect 2006;8:1339–1346. [PubMed: 16697232]

Jiao X, Lo-Man R, Guermonprez P, Fiette L, Deriaud E, Burgaud S, et al. Dendritic cells are host cells for mycobacteria *in vivo* that trigger innate and acquired immunity. J Immunol 2002;168:1294–1301. [PubMed: 11801668]

de Jonge MI, Pehau-Arnaudet G, Fretz MM, Romain F, Bottai D, Brodin P, et al. ESAT-6 from *Mycobacterium tuberculosis* dissociates from its putative chaperone CFP-10 under acidic conditions and exhibits membranelysing activity. J Bacteriol 2007;189:6028–6034. [PubMed: 17557817]

Junqueira-Kipnis AP, Basaraba RJ, Gruppo V, Palanisamy G, Turner OC, Hsu T, et al. Mycobacteria lacking the RD1 region do not induce necrosis in the lungs of mice lacking interferon-gamma. Immunology 2006;119:224–231. [PubMed: 17005003]

Kaneshiro, ES. Encyclopedia of Life Sciences. John Wiley & Sons; Chichester: Apr. 2001 Pneumocystis.. doi:10.1038/npg.els.0002101

Kinhikar A, Vargas D, Li H, Mahaffey SB, Hinds L, Belisle JT, Laal S. *Mycobacterium tuberculosis* malate synthase is a laminin binding adhesin. Mol Microbiol 2006;60:999–1013. [PubMed: 16677310]

Kocincova D, Sonden B, de Mendonca-Lima L, Gicquel B, Reyrat JM. The Erp protein is anchored at the surface by a carboxy-terminal hydrophobic domain and is important for cell-wall structure in *Mycobacterium smegmatis*. FEMS Microbiol Lett 2004;231:191–196. [PubMed: 14987764]

Lewis KN, Liao R, Guinn KM, Hickey MJ, Smith S, Behr MA, Sherman DR. Deletion of RD1 from *Mycobacterium tuberculosis* mimics Bacille Calmette-Guerin attenuation. J Infect Dis 2003;187:117–123. [PubMed: 12508154]

Lin Y, Zhang M, Barnes PF. Chemokine production by human alveolar epithelial cell line in response to *Mycobacterium tuberculosis*. Infect Immun 1998;66:1121–1126. [PubMed: 9488404]

Liu F, Chen H, Galvan EM, Lasaro MA, Schifferli DM. Effects of Psa and F1 on the adhesive and invasive interactions of *Yersinia pestis* with human respiratory tract epithelial cells. Infect Immun 2006;74:5636–5644. [PubMed: 16988239]

McDonough Kathleen A, Kress Y. Cytotoxicity for lung epithelial cells is a virulence-associated phenotype of *Mycobacterium tuberculosis*. Infect Immun 1995;63:4802–4811. [PubMed: 7591139]

McMurray DN. Hematogenous reseeding of the lung in low-dose, aerosol-infected guinea pigs: unique features of the host–pathogen interface in secondary tubercles. Tuberculosis (Edinb) 2003;83:131–134. [PubMed: 12758202]

Majlessi L, Brodin P, Brosch R, Rojas MJ, Khun H, Huerre M, et al. Influence of ESAT-6 secretion system 1 (RD1) of *Mycobacterium tuberculosis* on the interaction between mycobacteria and the host immune system. J Immunol 2005;174:3570–3579. [PubMed: 15749894]

Mehta PK, Karls RK, White EH, Ades EW, Quinn FD. Entry and intracellular replication of *Mycobacterium tuberculosis* in cultured human microvascular endothelial cells. Microb Pathog 2006;41:119–124. [PubMed: 16860530]

Menozzi FD, Reddy VM, Cayet D, Raze D, Debrie AS, Dehouck MP, et al. *Mycobacterium tuberculosis* heparin-binding haemagglutinin adhesin (HBHA) triggers receptor-mediated transcytosis without altering the integrity of tight junctions. Microbes Infect 2005;8:1–9. [PubMed: 15914062]

Nakamura Y, Wada M. Molecular pathobiology and antigenic variation of *Pneumocystis carinii*. Adv Parasitol 1998;41:63–107. [PubMed: 9734292]

Pierce RA, Griffin GL, Mudd MS, Moxley MA, Longmore WJ, Sanes JR, et al. Expression of laminin alpha3, alpha4, and alpha5 chains by alveolar epithelial cells and fibroblasts. Am J Respir Cell Mol Biol 1998;19:237–244. [PubMed: 9698595]

Pym AS, Brodin P, Brosch R, Huerre M, Cole ST. Loss of RD1 contributed to the attenuation of the live tuberculosis vaccines *Mycobacterium bovis* BCG and *Mycobacterium microti*. Mol Microbiol 2002;46:709–717. [PubMed: 12410828]

Rennard SI, Bitterman PB, Crystal RG. Response of the lower respiratory tract to injury. Mechanisms of repair of the parenchymal cells of the alveolar wall. Chest 1983;84:735–739. [PubMed: 6357653]

Renshaw PS, Panagiotidou P, Whelan A, Gordon SV, Hewinson RG, Williamson RA, Carr MD. Conclusive evidence that the major T-cell antigens of the *Mycobacterium tuberculosis* complex ESAT-6 and CFP-10 form a tight, 1:1 complex and characterization of the structural properties of ESAT-6, CFP-10, and the ESAT-6*CFP-10 complex. Implications for pathogenesis and virulence. J Biol Chem 2002;277:21598–21603. [PubMed: 11940590]

Renshaw PS, Lightbody KL, Veverka V, Muskett FW, Kelly G, Frenkiel TA, et al. Structure and function of the complex formed by the tuberculosis virulence factors CFP-10 and ESAT-6. EMBO J 2005;24:2491–2498. [PubMed: 15973432]

Rogerson BJ, Jung YJ, LaCourse R, Ryan L, Enright N, North RJ. Expression levels of *Mycobacterium tuberculosis* antigen-encoding genes versus production levels of antigen-specific T cells during stationary level lung infection in mice. Immunol 2006;118:195–201.

Rubins JB, Janoff EN. Pneumolysin: a multifunctional pneumococcal virulence factor. J Lab Clin Med 1998;131:21–27. [PubMed: 9452123]

Rubins JB, Duane PG, Clawson D, Charboneau D, Young J, Niewoehner DE. Toxicity of pneumolysin to pulmonary alveolar epithelial cells. Infect Immun 1993;61:1352–1358. [PubMed: 8454338]

Rubins JB, Paddock AH, Charboneau D, Berry AM, Paton JC, Janoff EN. Pneumolysin in pneumococcal adherence and colonization. Microb Pathog 1998;25:337–342. [PubMed: 9895272]

Smith J, Manoranjan J, Pan M, Bohsali A, Xu J, Liu J, et al. Evidence for pore formation in host cell membranes by ESX-1-secreted ESAT-6 and its role in *Mycobacterium marinum* escape from the vacuole. Infect Immun 2008;76:5478–5487. [PubMed: 18852239]

Tailleux L, Schwartz O, Herrmann JL, Pivert E, Jackson M, Amara A, et al. DC-SIGN is the major *Mycobacterium tuberculosis* receptor on human dendritic cells. J Exp Med 2003;197:121–127. [PubMed: 12515819]

Teitelbaum R, Schubert W, Gunther L, Kress Y, Macaluso F, Pollard JW, et al. The M cell as a portal of entry to the lung for the bacterial pathogen *Mycobacterium tuberculosis*. Immunity 1999;10:641–650. [PubMed: 10403639]

Vir, P.; Gupta, D.; Verma, I. Tuberculosis: Biology, Pathology and Therapy. Keystone Symposia on Molecular and Cellular Biology; Keystone, CO: 2009. Interaction of *Mycobacterium tuberculosis* with type I alveolar epithelial cells.; p. 151

van der Wel N, Hava D, Houben D, Fluitsma D, van Zon M, Pierson J, et al. *M. tuberculosis* and *M. leprae* translocate from the phagolysosome to the cytosol in myeloid cells. Cell 2007;129:1287–1298. [PubMed: 17604718]

Wu CH, Tsai-Wu JJ, Huang YT, Lin CY, Lioua GG, Lee FJ. Identification and subcellular localization of a novel Cu,Zn superoxide dismutase of *Mycobacterium tuberculosis*. FEBS Lett 1998;439:192–196. [PubMed: 9849904]

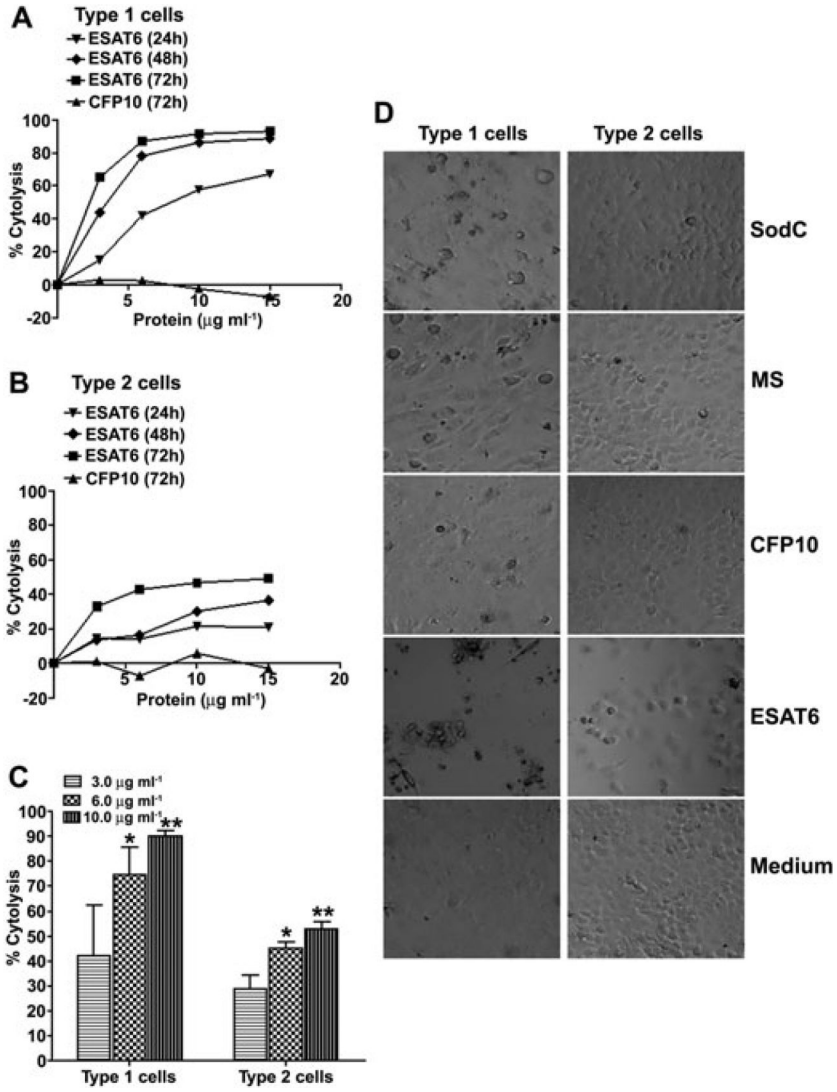

Fig. 1.

ESAT6 causes dose- and time-dependent cytolysis of type 1 and 2 pneumocytes.

A and B. (A) Type 1 pneumocytes (WI26 cells) and (B) type 2 pneumocytes (A549 cells) were incubated with several concentrations of ESAT6 or CFP10 for 24, 48 and 72 h at which time MTT assay was performed to quantify lysis. Cells exposed to medium alone were used as controls; each assay condition was tested in six wells. Per cent cytolysis was calculated by using the formula: (Mean OD_{530} of 6 control wells – Mean OD_{530} of 6 test wells)/(Mean OD_{530} of 6 control wells) × 100. For CFP10, only results obtained at 72 h are shown. These assays were done atleast 3 times and a single representative assay with each cell line is shown.

C. Type 1 pneumocytes are significantly more sensitive to ESAT6-mediated cytolysis than type 2 pneumocytes at 6 μg ml^{-1} (*P = 0.0098) and 10 μg ml^{-1} (**P = 0.0005) of ESAT6. Per cent cytolysis obtained after 72 h of incubation of the two cell lines with different concentrations of ESAT6 is plotted. Values are mean percentage cytolysis ± SD from at least three independent experiments.

D. Microscopic visualization of cytolysis of type 1 and 2 pneumocytes when exposed to 10 μg ml^{-1} *M. tb* proteins for 72 h. Cells were visualized using a Nikon microscope at 100× magnification. Photographs shown are digitally magnified to show the monolayers.

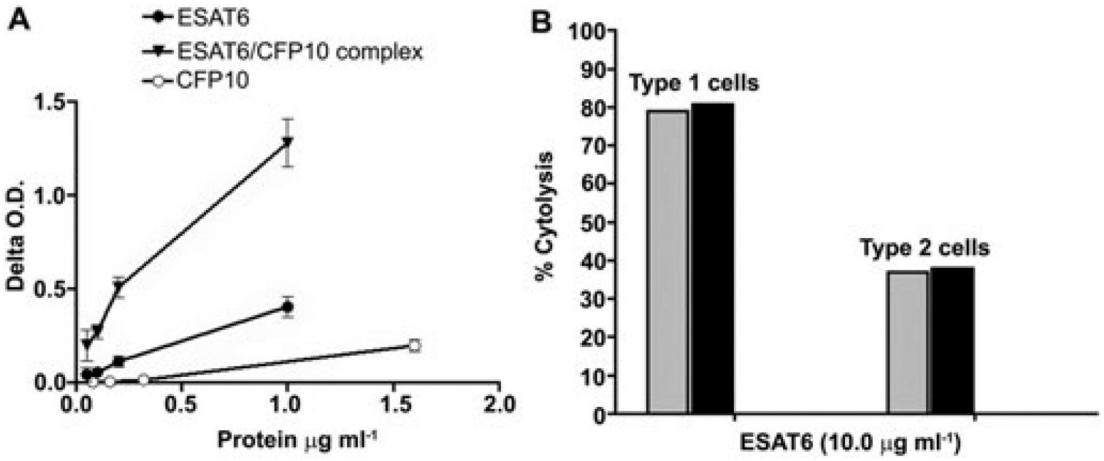

Fig. 2.

ESAT6 causes cytolysis of type 1 and 2 pneumocytes when complexed with CFP10.

A. Confirmation of complex formation: Various dilutions of a 1:1 molar mixture of ESAT6 and CFP10 (containing 1, 0.2, 0.1 and 0.05 μg ml^{-1} of ESAT6) were added to anti-CFP10 IgG coated wells, as were the same concentrations of ESAT6 or CFP10 alone and detected with anti-ESAT6 IgG. The Delta OD_{490} (mean OD_{490} with anti-ESAT6 IgG at each concentration of the complex or the individual protein minus the mean OD_{490} in wells exposed to anti-ESAT6 IgG) is plotted. Immune complexes captured by anti-CFP10 and detected by anti-ESAT6 antibodies were present at all dilutions of the ESAT6 and CFP10 mixture.

B. Cytolysis of type 1 and type 2 pneumocytes with ESAT6:CFP10 complexes (black bars) or by ESAT6 alone (grey bars). Both experiments were done twice with 3–6 replicates providing similar results and one representative experiment is shown.

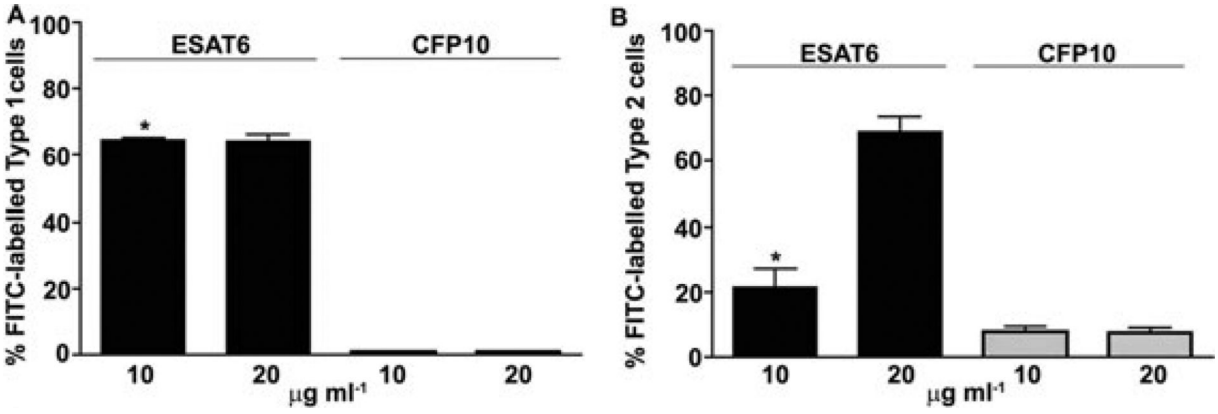

Fig. 3.

Binding of ESAT6 and CFP10 to type 1 and type 2 pneumocytes. (A) WI26 cells or (B) A549 cells were incubated with ESAT6 or CFP10 (10 or 20 μg ml^{-1}) or buffer (in triplicates) followed by exposure to anti-His antibodies and FITC-conjugated secondary antibodies were analysed by FACS. Only ESAT6 showed binding to the two cell types. The per cent FITC-labelled cells obtained when cells were incubated with either protein minus per cent FITC labelled cells exposed to anti-His antibodies and FITC-conjugated secondary antibody from a representative experiment is shown. The binding of ESAT6 to type 1 pneumocytes was significantly higher than type 2 cells at 10 μg ml^{-1} (*P = 0.032) and similar at 20 μg ml^{-1}.

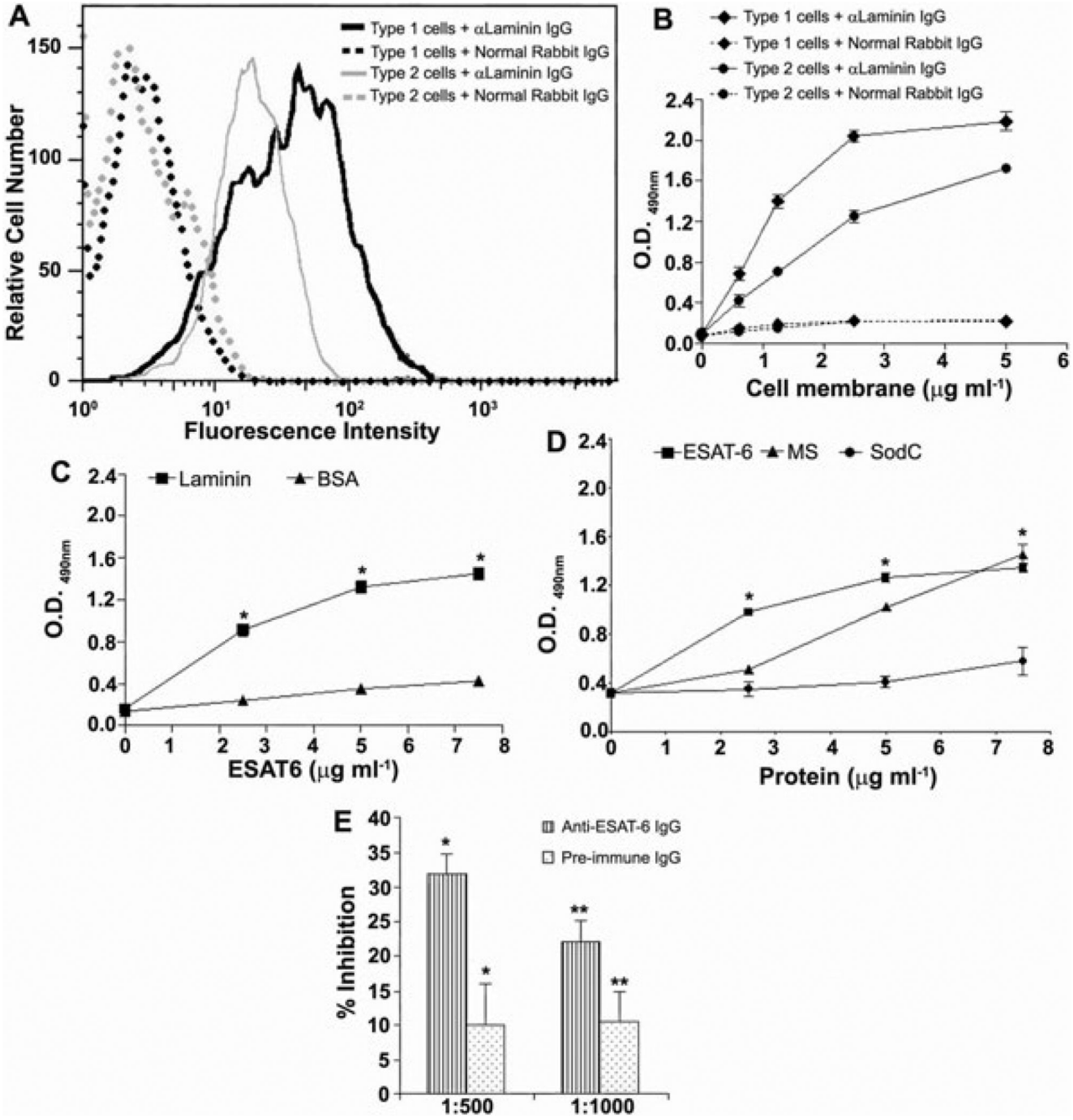

Fig. 4.

Presence of laminin on the surface of type 1 and type 2 pneumocytes.

A. Cells were exposed to anti-laminin antibodies or normal rabbit antibodies followed by FITC-conjugated anti-rabbit antibodies. Type 1 pneumocytes have more laminin/cell than type 2 pneumocytes. Cells were exposed to each antibody in triplicates and the experiment was done two times.

B. Detection of laminin in membrane preparations of cells. Different concentrations of the membrane preparations were tested in triplicates and the experiment was performed twice with similar results. The OD values (mean ± SD) from one representative experiment are plotted.

C. ESAT6 binds to purified laminin: increasing concentrations of ESAT6 were added to wells coated with laminin or BSA at 1 μg ml^{-1} and the binding of ESAT6 detected with anti-ESAT6 IgG. Each condition was tested in triplicate and the experiment was performed twice with similar results. Values (mean ± SD) from one representative experiment are plotted. As compared with BSA the binding of ESAT6 to laminin was significantly higher at all concentrations tested (*$P < 0.0001$).

D. Specific binding of ESAT6 to laminin: various concentrations of His-tagged *M. tb* proteins (ESAT6, MS and SodC) were incubated with laminin (1 μg ml^{-1}) coated wells and binding of *M. tb* proteins was detected with anti-His mAbs. Compared with SodC, the binding of ESAT6 to laminin was significantly higher at all concentrations tested (*$P < 0.0001$).

E. Inhibition of binding of ESAT6 to laminin by anti-ESAT6 IgG. ESAT6 preincubated with anti-ESAT6 IgG (striped bars) or pre-immune IgG (dotted bars) was added to laminin-coated wells (in triplicates) and the laminin-bound ESAT6 was detected by anti-His IgG. Per cent inhibition of binding of ESAT6 to laminin from one representative experiment is plotted. Inhibition of ESAT6–laminin interaction by anti-ESAT6 IgG was significantly higher compared with inhibition by pre-immune IgG at both dilutions tested (*$P = 0.009$ at 1:500 and **$P = 0.037$ at 1:1000).

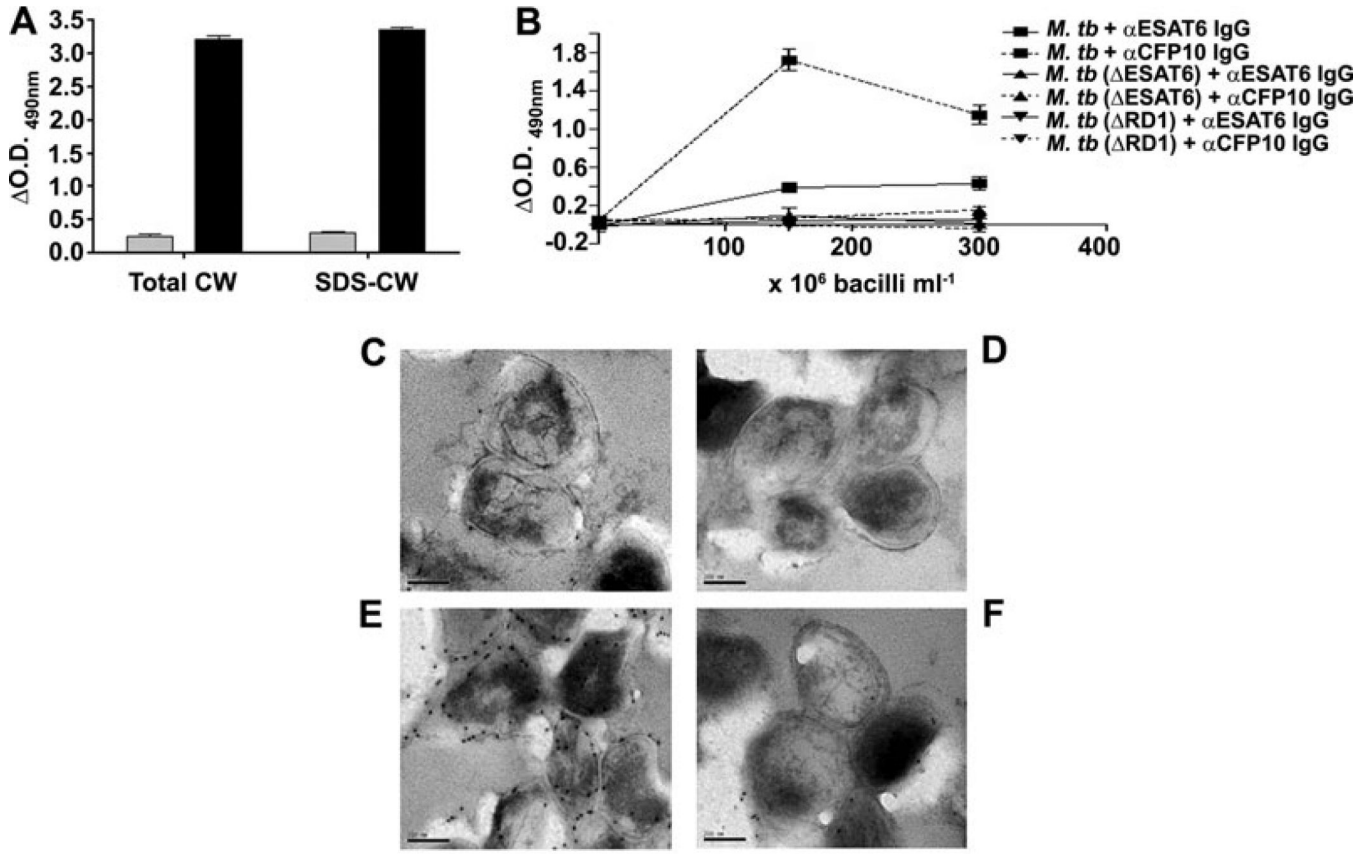

Fig. 5.

Paucity of ESAT6 in and on the *M. tb* cell wall.

A. *M. tb* cell wall preparations were tested for presence of ESAT6 (grey bars) or CFP10 (black bars) by ELISA with respective antibodies.

B. γ-Irradiated *M. tb* $H_{37}Rv$, $H_{37}Rv$:ΔESAT6 and $H_{37}Rv$:ΔRD1 were coated at various concentrations in ELISA plates and the respective antibodies used to detect ESAT6 or CFP10 on the surface of the intact bacterial cells. ΔOD_{490} = Mean OD_{490} with anti-protein IgG at any protein/bacterial concentration – OD_{490} with pre-immune IgG at the same concentration.

C–F. Immunoelectron microscopy of ultrathin sections of γ-irradiated *M. tb* probed with anti-ESAT6 IgG (C), pre-immune IgG from the ESAT-6 immunized animal (D), anti-CFP10 IgG (E) and pre-immune IgG (F) from the CFP10 immunized animal.

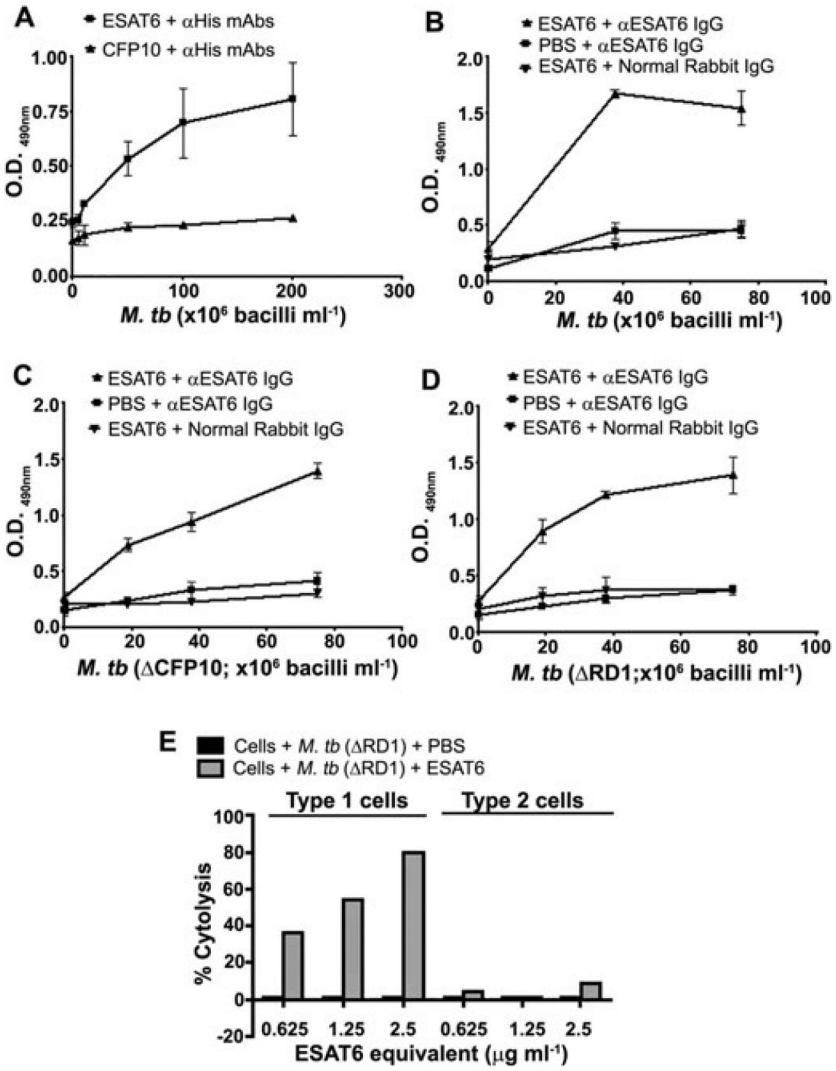

Fig. 6.

Association of exogenous ESAT6 with *M. tb* cell surface.

A. Re-association of exogenously added His-tagged ESAT6 or CFP10 (2 μg ml^{-1}) with *M. tb* $H_{37}Rv$ surface as detected by anti-His Abs.

B–D. Re-association of ESAT6 with surface of *M. tb* $H_{37}Rv$ (B), *M. tb* $H_{37}Rv$:Δ*cfp10* (C) or *M. tb* $H_{37}Rv$:Δ*RD1* (D) as detected by anti-ESAT6 IgG.

E. Cell surface associated ESAT6 is cytolytic. Type 1 pneumocytes and type 2 pneumocytes incubated with various dilutions of γ-irradiated *M. tb* $H_{37}Rv$:Δ*RD1* carrying reassociated ESAT6 for 72 h were tested by MTT assay for cytolysis and mean OD_{530} from 3 replicates at each concentration were used to calculate the per cent cytolysis.

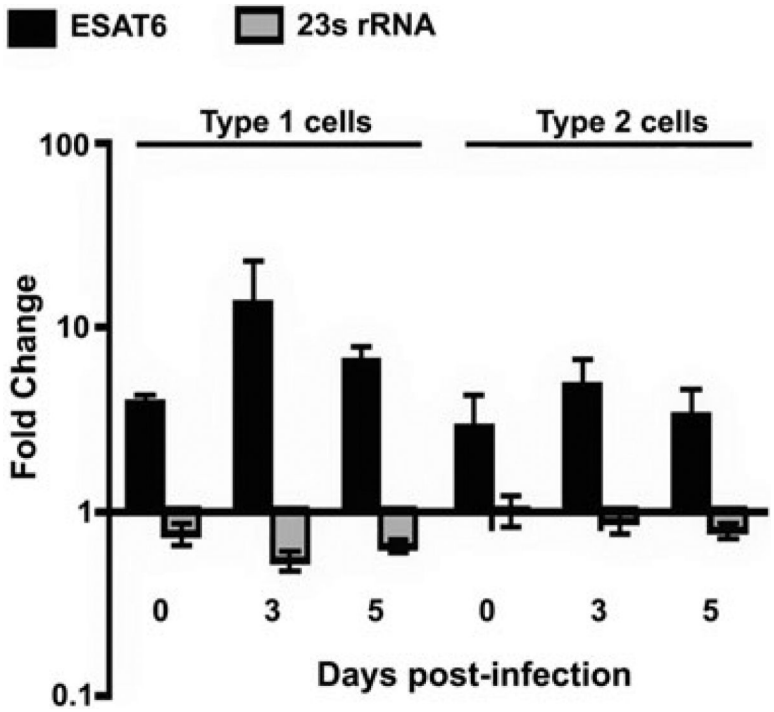

Fig. 7.

esat6 transcripts are upregulated in *M. tb* replicating in type 1 and 2 pneumocytes. The fold change (ratios of copies of *esat6* or 23S rRNA normalized to 16S rRNA copies in bacteria from type 1 or 2 pneumocytes to the normalized copies of respective genes in broth grown bacteria) ± standard deviation (error bars) from triplicates of a representative of two experiments are shown.